

## A Study on the Merging Position of Frozen Layers in Injection-Molded Disks and Rectangular Plates

**Kyunghwan Yoon\***

*(Received March 29, 1996)*

Thermal and flow simulations of center-gated disks and rectangular plates molded under different process conditions are presented. The process variables were melt temperature, mold temperature, injection speed and packing pressures which have been varied systematically. The input pressure data were taken from the experimental traces, if possible. In particular, we have focused on the effect of process conditions on the growth of, so called, a frozen layer. We found that the frozen layer started to merge at about  $0.75R$  from the center for the center-gated disks and about  $0.25 - 0.35 L$  from the gate for the rectangular plates for most of process conditions. The present result would help to understand the mechanism how the packing process affects the limited portion in overpacked injection-molded parts.

**Key Words :** Injection Molding, Optical Disk, Numerical Simulation, Frozen Layer

### 1. Introduction

Injection molding is one of the most popular processes in the plastic industry. The process consists of heating the plastic material to above the melting temperature, injecting the melt into a cold mold and packing extra material to compensate volumetric shrinkage of the final part. Usually the whole process can be divided into three stages, namely, filling, packing and cooling stages. Even though the filling and packing stages can be separated clearly, the cooling stage continues through the whole process. During the process the polymer melt flows through the thin gap in a cold mold. Because the polymer melt shows non-Newtonian behavior and experiences the differential cooling with phase change, an accurate analysis of the whole injection molding process is rather difficult to achieve.

Since Gilmore and Spencer (1950 & 1951) started to investigate the process scientifically, numerous experimental and numerical studies have been performed relating various aspects of

the process. Kamal and Kenig (1972) used a finite difference numerical simulation to implement the process for the first time. Recently, a finite element method for planar direction and a finite difference method for gapwise direction have been widely used for solving the equations given for more complex geometry. (Bernhardt, 1983; Isayev, 1987; Manzoine, 1987) Up to now, most of analyses available for cavity filling have been based on non-isothermal flow of a generalized Newtonian fluid (Isayev, 1987).

Later on, an analysis for the packing stage has been performed based on the weakly compressible fluid model by incorporating melt compressibility into the formulation. (Chiang, Hieber and Wang, 1991a, b) Recently Huilier et al. (1990 and 1991) gave a comprehensive review on the simulation of a packing stage. However, it has been well known that inelastic analyses could not provide information about frozen-in stresses and orientations even for the simple geometry. This stimulated the researchers to pay more attention to viscoelastic modeling of the injection molding process. Isayev and Hieber (1980) used Leonov model (Leonov et al. ; 1976, Leonov, 1976) for the simulation of viscoelastic melt in a strip cavity. Their prediction for the final flow-induced stresses and birefrin-

---

\* Department of Mechanical Engineering, Dankook University San 8, Hannam-dong, Yongsan-ku, Seoul 140-714, Korea

gece was quite acceptable. Also Isayev(1991) continued to apply the same approach to a center-gated disk, too. However, all the previous viscoelastic calculations did not include a packing stage in the simulation.

Baaijens (1991) introduced the compressible version of Leonov model to both filling and postfilling stages for the first time. Later, Flaman (1993 a & b) applied this model to the whole injection molding process and showed good agreement between the predicted and experimental values of the flow induced birefringence for the strip.

In the present study we will show the thermal and flow history in the injection-molded center-gated disks and rectangular plates for the whole process including packing and cooling stages. For the first time we will show that the merging position of a frozen layer for different geometries can be changed dramatically. The former researchers paid their attention only for the early stages in the process. However, our results came from the extension of the calculation until it met at the center in the thickness direction. Finally we will show how the present results could be correlated with the overpacking phenomenon.

## 2. Theoretical Analysis

### 2.1 Governing equations and boundary conditions

The governing Equations for a compressible, non-isothermal fluid flow without body force are as follows(Isayev and Hieber; 1980) :

$$\frac{\partial \rho}{\partial t} + \nabla \cdot (\rho \vec{v}) = 0 \quad (1)$$

$$\rho \left( \frac{\partial \vec{v}}{\partial t} + \vec{v} \cdot \nabla \vec{v} \right) = -\nabla p - \nabla \cdot \underline{\underline{\tau}} \quad (2)$$

$$\rho C_p \left( \frac{\partial T}{\partial t} + \vec{v} \cdot \nabla T \right) = k \nabla^2 T + \phi \quad (3)$$

$$\underline{\underline{\tau}} = \eta_0 s \{ \nabla \vec{v} + (\nabla \vec{v})^T \} + \sum_{k=1}^N \frac{\eta_k}{\theta_k} \underline{\underline{C}}_k \quad (4)$$

In the above equations  $\vec{v}$  is the velocity vector,  $\underline{\underline{\tau}}$  is the stress tensor where Leonov model (4) is selected,  $p$  is the pressure,  $\underline{\underline{C}}_k$  is the elastic Finger strain tensor,  $\phi$  is the dissipation function,  $\theta_k(T)$  and  $\eta_k(T)$  are the relaxation time and shear visc-

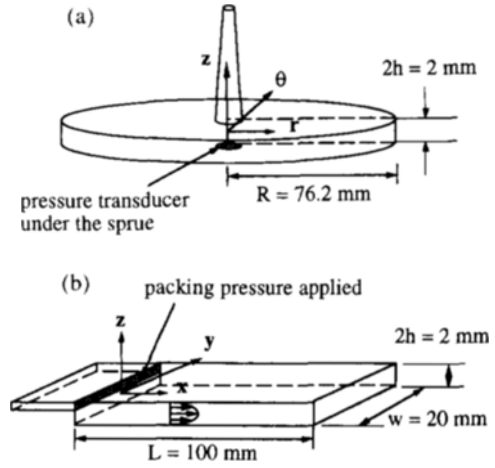


Fig. 1 The coordinate system chosen for a center-gated disk (a) and a rectangular plate (b)

osity of the  $k$ -th mode at a given temperature  $T$ , respectively.

While the coordinate system of a center-gated disk was chosen as in Fig. 1 (a), following boundary conditions were applied to solve the given equations.

$$u_r = u_z = 0 \text{ and } T = T_w \text{ at } z = \pm h \quad (5)$$

$$\frac{\partial u_r}{\partial z} = \frac{\partial T}{\partial z} = 0 \text{ and } u_z = 0 \text{ at } z = 0 \quad (6)$$

where  $u_r$  and  $u_z$  are the velocities for radial and thickness direction, respectively, and  $T_w$  is the constant mold wall temperature.

For the rectangular plate shown in Fig. 1 (b), the same boundary conditions of Eqs. (7) and (8) were applied as above.

$$u = w = 0 \text{ and } T = T_w \text{ at } z = \pm h \quad (7)$$

$$\frac{\partial u}{\partial z} = \frac{\partial T}{\partial z} = 0 \text{ and } w = 0 \text{ at } z = 0 \quad (8)$$

where  $u$  and  $w$  are the velocities for flow and thickness direction, respectively.

In the packing stage the pressure at the center of the disk was taken from the experiment if possible, and impermeable conditions ( $\partial p / \partial r = 0$ ) was applied at the outer edge of the wall. For the rectangular plate the pressure at the gate was taken constant ideally after the end of filling process. An impermeable condition ( $\partial p / \partial x = 0$ )

was applied at the end wall as in the case of a center-gated disk.

**2.2 Numerical method**

A standard finite difference method (Patankar, 1980) was applied to solve the Eqs. (1) ~ (4). From the filling to the packing stage Leonov's model was used for the shear viscosity. Especially, for the flow direction a staggered mesh was adopted to cover the center of the disk. 50 meshes in the flow direction and 18 meshes in the thickness direction were chosen for both center-gated disks and a rectangular plate. In the packing stage the Eqs. (1) and (2) were solved simultaneously (Wang, et al., 1992).

**2.3 Molding conditions**

From the previous experience (Yoon and Wang, 1992) a melt temperature of 225°C, a mold temperature of 40°C and an injection speed of 23.8 cc/sec were chosen as a reference molding condition for both center-gated disk and a rectangular plate. The holding (hydraulic ram) pressure was kept constant of 2.07 MPa for the reference molding condition.

In this series of experiments melt temperature, flow rate and packing pressure were varied to find the effect of molding conditions on the formation of a frozen layer. Hence the pressure trace at the center of the disk was needed as an input data, the pressure traces taken from flush mounted Dynisco pressure transducer (465XL) under the sprue was used, if possible.

The diameter of the disk was 152.4mm and the nominal thickness was 2.0mm. The length and width of the rectangular plate were taken as 100 mm and 20mm. The nominal thickness was 2.0 mm for the reference condition which is the same as for the center-gated disk. All the samples were

**Table 1** Leonov model constants

	Mode 1	Mode 2
$\theta_k$ (sec)	$4.230 \times 10^{-2}$	$9.295 \times 10^{-4}$
$\eta_k$ (dynes-sec/cm <sup>2</sup> )	$1.351 \times 10^4$	$8.679 \times 10^{-2}$

made of polystyrene, Dow Styron 615APR.

**2.4 Material property data**

The detailed property data such as viscosity, thermal conductivity and specific volume for Dow Styron 615APR were taken from Wang, et al.(1992) as follows.

A two-mode Leonov model for the steady shear viscosity in Eq.(9) has been used along with the constants from Table 1.

$$\eta = \eta_0 s + \sum_{k=1}^N \frac{2\eta_k}{1 + q_k} \tag{9}$$

where  $q_k = \sqrt{1 + 4\gamma^2 \theta_k^2}$  and s is the constant for the second Newtonian region which has been taken as  $1.835 \times 10^{-3}$ .

And the zero-shear viscosity  $\eta_0$  was modeled as in Eq.(10).

$$\eta_0(T, p) = D_1 \exp\left(-\frac{A_1(T - T^*)}{A_2 + (T - T^*)}\right) \tag{10}$$

where the transition temperature  $T^*(p) = D_2 + D_3 p$  and  $A_2 = \tilde{A}_2 + D_3 p$ .

**Table 2** The constants in a shift function

A <sub>1</sub>	A <sub>2</sub> (°C)	D <sub>2</sub> (°C)	D <sub>3</sub> (°C - cm <sup>2</sup> /dyne)
22.51	60	100	$2.30 \times 10^{-8}$

The density has been assumed to obey a double-domain Tait equation as in Eqs.(11) ~ (13) with the constants shown in Table 3.

**Table 3** Constants for the double-domain Tait equation

B <sub>1</sub> (cm <sup>3</sup> /g)	B <sub>2</sub> (cm <sup>3</sup> / g·°C )	B <sub>3</sub> (dyne/ cm <sup>2</sup> )	B <sub>4</sub> (°C <sup>-1</sup> )	B <sub>5</sub> (°C)
1.0071	$5.789 \times 10^{-4}$	$2.021 \times 10^9$	$3.009 \times 10^{-3}$	150
B' <sub>1</sub> (cm <sup>3</sup> /g)	B' <sub>2</sub> (cm <sup>3</sup> / g·°C )	B' <sub>3</sub> (dyne/ cm <sup>2</sup> )	B' <sub>4</sub> (°C <sup>-1</sup> )	
0.9892	$2.422 \times 10^{-4}$	$2.260 \times 10^9$	$1.363 \times 10^{-3}$	

**Table 4** Measured specific heat capacity and thermal conductivity

T(°C)	Cp(erg/g-°C)	T(°C)	k(erg/g-cm-°C)
0	$1.11 \times 10^7$	0	$1.20 \times 10^4$
66	$1.38 \times 10^7$	160	$1.75 \times 10^4$
100	$1.83 \times 10^7$	300	$1.75 \times 10^4$
240	$2.24 \times 10^7$		

$$\rho(T, p) = \left[ v_0(T) \left\{ 1 - C \ln \left( 1 + \frac{p}{B(T)} \right) \right\} \right]^{-1} \quad (11)$$

$$v_0(T) = B_1 + B_2 T \quad \text{if } T > T_i \quad (12)$$

$$B'_1 + B'_2 T \quad \text{if } T < T_i$$

$$B(T) = B_3 \exp(-B_4 \bar{T}) \quad \text{if } T < T_i \quad (13)$$

$$B'_3 \exp(-B'_4 \bar{T}) \quad \text{if } T < T_i$$

where  $\bar{T} = T - B_5$  and  $T_i = B_5 + B_5 p$

The specific heat capacity and thermal conductivity have been linearized as a function of temperature through the experimental values shown in Table 4.

### 3. Results

Since the results from the thermal and flow history for different cases are very similar, the detailed gapwise distribution of the velocity, shear rate and temperature during filling and packing stages are presented only for the center-gated disk and for a reference condition at a specific location (30 mm from the gate). Only the final merging position of frozen layers are compared for other process conditions and for the case of rectangular plates.

#### 3.1 Filling stage

Figure 2 shows the gapwise distribution of the radial velocity, shear rate and temperature history during the filling stage at a given radial location 30 mm apart from the center of the disk cavity for the reference condition as shown in the section 2.3. Figure 2(a) shows that the radial velocity near  $z/h=0$  increases as time progresses. This is due to the solidification of the liquid polymer

near the mold wall surface as shown in Fig. 2(c). Also it is noticed that the location of shear rate maximum moves to the center of the cavity gap as shown in Fig. 2(b).

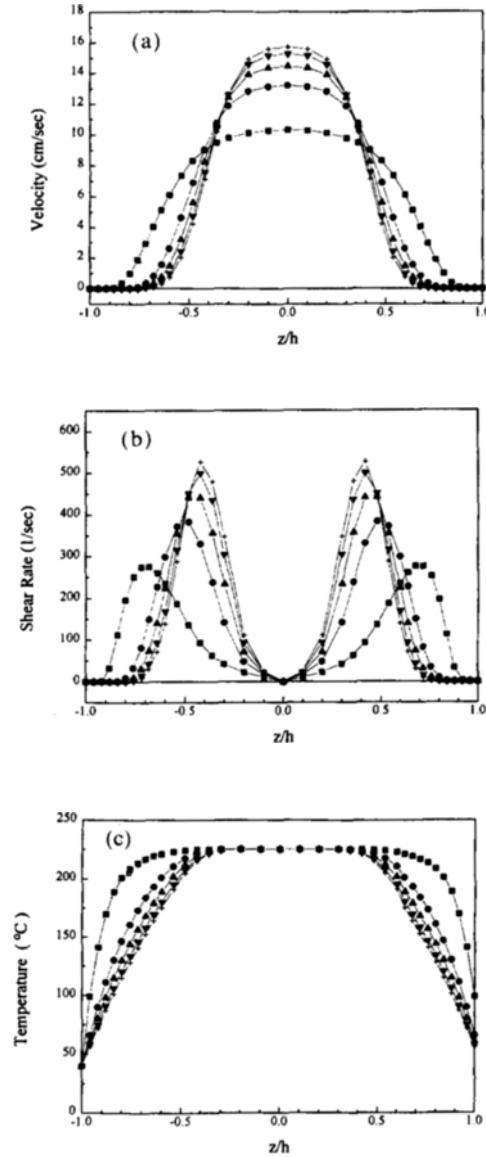


**Fig. 2** The gapwise distribution of radial velocity (a), shear rate (b) and temperature (c) for a center-gated disk during filling (case 1). (Symbols  $\blacksquare$ ,  $\bullet$ ,  $\blacktriangle$ ,  $\blacktriangledown$ ,  $+$  denote the time 0.328, 0.637, 0.902, 1.213 and 1.571 seconds after the start of filling.)

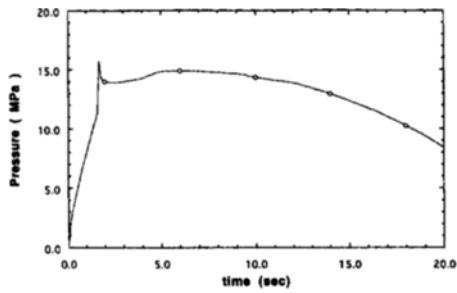


Fig. 3 A pressure history at the center of the disk mold for the reference condition(case 1).

**3.2 Packing stage**

The pressure history under the sprue for the reference condition is shown in Fig. 3, which is taken from the experiment and used as an input data for the packing simulation.

Figure 4(a),(b) and(c) show the gapwise distribution of the radial velocity, shear rate and temperature histories, respectively, during the packing stage at a given radial location 30 mm apart from the center of the disk cavity for the reference case. Figure 4(a) shows that the radial velocity decreases as time progress because the polymer cools down rapidly as shown in Fig. 4(c). Notice that, in the packing stage, the radial velocity and shear rate are much lower than the filling stage. This happens because the hydraulic pressure on the backside of the injection screw is controlled in the packing stage rather than controlling the screw speed in the filling stage and cooling progresses further.

**3.3 Frozen layer growth**

An interesting fact could be found when the isotherms of some specific temperatures were plotted as a function of time. When Janeschitz-Kriegl (1977) formulated the mold filling process as an ideal heat transfer problem, he introduced the “solidified layer” below a temperature  $T_1$  at which the polymer stops flowing. The viscosity at the temperature  $T_1$  was defined  $e$  (exponent, 2.71828) times of the viscosity at the injection temperature. For polystyrene  $T_1$  was chosen  $70^\circ\text{C}$  lower than the injection tempera-

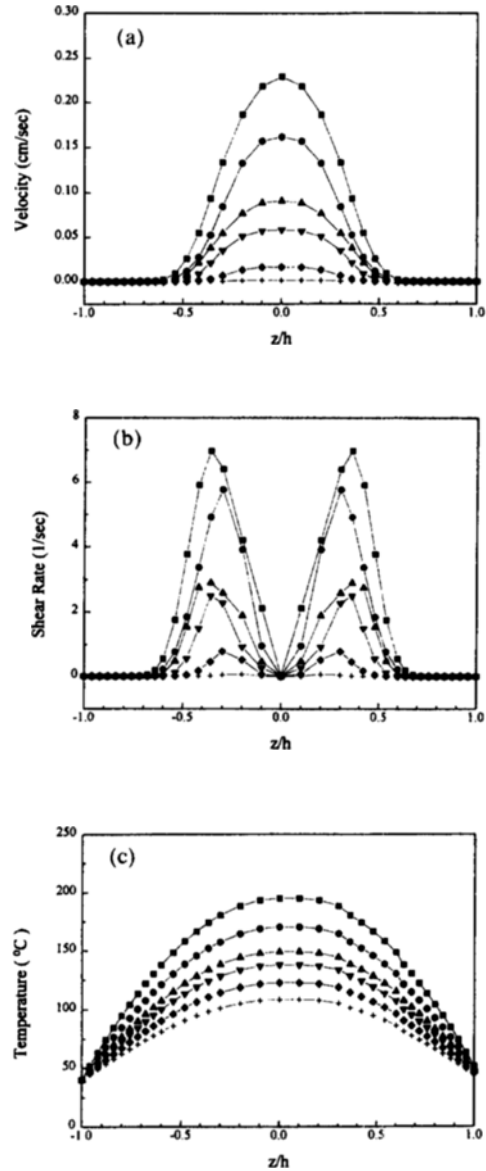


Fig. 4 The gapwise distribution of radial velocity (a), shear rate(b) and temperature(c) during packing for a center-gated disk (case 1). (Symbols  $\blacksquare$ ,  $\bullet$ ,  $\blacktriangle$ ,  $\blacktriangledown$ ,  $\blacklozenge$ ,  $+$  denote the time 1.1, 2.1, 3.1, 4.1, 5.0 and 6.0 seconds after the end of filling.)

ture. And he investigated the growth of the “solidified layer” as a function of time at any distance from the gate. However, his choice for the temperature  $T_1$  seems to be too high for the

polymer to stop flowing.

Isayev (1987) had chosen the temperature of stop flowing as a glass transition temperature  $T_g$  and showed the growth of the "solidified layer" as a function of time during a filling process. But his data for the "solidified layer" only covered until the end of fill. At the end of fill the "solidified layer" did not close the gap in the cavity.

In the present paper  $100^\circ\text{C}$  was taken as one of the reference temperatures because it was the glass transition temperature of polystyrene. And another temperature  $130^\circ\text{C}$  was chosen to draw the isotherms because it was known as a "no-flow temperature" (Santhanam, 1992). Below these temperatures the polymer can be treated as a viscoelastic solid. Recently, this solidified skin is used to be called as a "frozen layer" rather than a "solidified layer".

Fig. 5(a) and (b) show the isotherms of  $100^\circ\text{C}$  and  $130^\circ\text{C}$ , respectively, for the center-gated disk at a reference condition. If we define the radial position for merging frozen layer as  $r_c$ , both isotherms of  $100^\circ\text{C}$  and  $130^\circ\text{C}$  meet at  $r_c/R=0.75$  from the center of the disk.

As the process conditions were varied as shown in Table 5, the following results were found.

When only the melt temperature  $T_M$  was changed as shown in the case 1 through 3, the first merging position of the frozen layers has not been

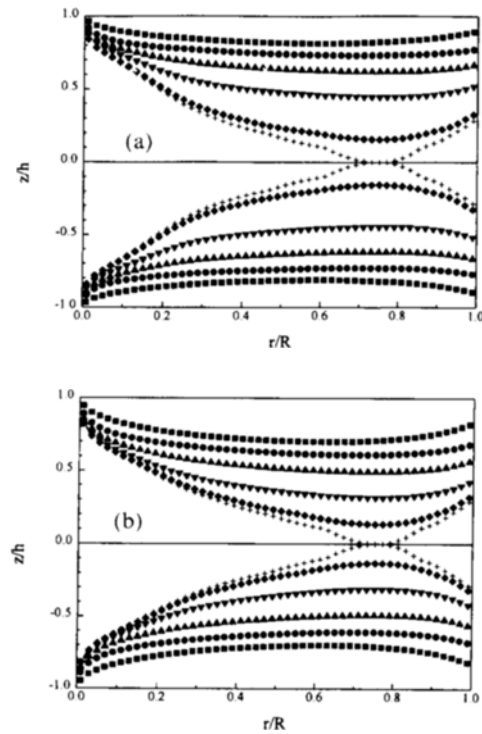
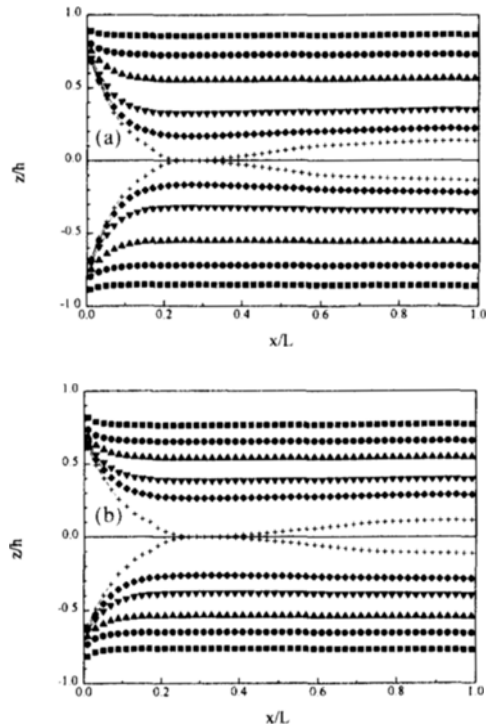


Fig. 5 The isotherms of  $100^\circ\text{C}$  (a) and  $130^\circ\text{C}$  (b) for a center-gated disk during packing (case 1). (Symbols  $\blacksquare$ ,  $\bullet$ ,  $\blacktriangle$ ,  $\blacktriangledown$ ,  $\blacklozenge$ ,  $+$  denote the time 0.60, 2.10, 3.60, 5.10, 6.30 and 6.468 seconds (a) and  $\blacksquare$ ,  $\bullet$ ,  $\blacktriangle$ ,  $\blacktriangledown$ ,  $\blacklozenge$ ,  $+$  denote the time 0.60, 1.60, 2.60, 3.60, 4.10 and 4.217 seconds (b) after the end of filling.)

Table 5 Molding conditions for center-gated disks.

Case No.	$T_M$ ( $^\circ\text{C}$ )	$T_w$ ( $^\circ\text{C}$ )	Flow Rate (cc/sec)	Packing pressure (MPa)	$100^\circ\text{C}$ ( $r_c/R$ )	$130^\circ\text{C}$ ( $r_c/R$ )
1	225	40	23.8	16.5	0.75	0.75
2	210	40	23.8	16.5	0.75	0.75
3	240	40	23.8	16.5	0.75	0.77
4	225	40	47.6	16.5	0.69	0.71
5	225	40	23.8	2.76	0.73	0.75
6	225	40	23.8	5.52	0.75	0.75
7	225	40	23.8	8.27	0.75	0.75
8	225	40	23.8	11.0	0.75	0.75
9	225	40	23.8	13.8	0.75	0.75
10	225	40	23.8	19.3	0.75	0.75
11	225	40	23.8	22.1	0.75	0.77



**Fig. 6** The isotherms of 100°C (a) and 130°C (b) for a rectangular plate during packing (case 1). (Symbols  $\blacksquare$ ,  $\bullet$ ,  $\blacktriangle$ ,  $\blacktriangledown$ ,  $\blacklozenge$ ,  $+$  denote the time 1, 10, 3, 10, 5, 10, 6, 60, 7, 10 and 7, 288 seconds (a) and  $\blacksquare$ ,  $\bullet$ ,  $\blacktriangle$ ,  $\blacktriangledown$ ,  $\blacklozenge$ ,  $+$  denote the time 1, 10, 2, 10, 3, 10, 4, 10, 4, 60 and 5, 034 seconds (b) after the end of filling.)

changed as  $r_c/R = 0.75$  for both 100°C and 130°C. For the case of  $T_M = 240^\circ\text{C}$  the first merging position of the frozen layers of 130°C occurred at  $r_c/R = 0.77$  which was only one mesh length (flow direction) apart from  $r_c/R = 0.75$ .

When the flow rate was increased twice as much as the one of the reference case (case 1)  $r_c/R$  has been decreased to 0.69 and 0.71 for 100°C and 130°C, respectively.

As the packing pressure was increased while the other parameters were kept constant as shown in the case 5 through 11, no appreciable effect has been found for the value for the first merging position of the frozen layers of both isotherms as shown in Table 5.

Note that the input pressure data for all the above cases for the center-gated disks were taken from the experiment.

Figure 6(a) and (b) show the isotherms of 100°C and 130°C, respectively, for the rectangular plate at a reference condition. If we define the longitudinal (flow direction) position for merging frozen layer as  $x_c$ , the isotherms of 100°C and 130°C meet at  $x_c/L = 0.27$  and  $x_c/L = 0.31$ , respectively, from the gate. Comparing with the results for the center-gated disks of  $r_c/R = 0.75$ , the first merging position of the frozen layers for the rectangular plate were much closer to the gate.

As the process conditions were varied systematically as shown in Table 6, the following results were found.

When the melt temperature  $T_M$  was changed, while the other parameters were kept constant, as shown in the case 1 through 3, the first merging position of the frozen layers has been increased for both 100°C and 130°C as  $T_M$  increased. However, the effect of the change of the melt temperature was somewhat minor. Here the packing pressure has been kept constant as the pressure for the gate at the end of fill of the cavity.

When the flow rate (or injection speed) was increased, while the other parameters were kept constant, as shown in the case 4 through 6, the first merging position of the frozen layers  $x_c/L$  has been decreased for both 100°C and 130°C. As for the cases of melt temperature the effect of the change of the flow rate to  $x_c/L$  was not significant.

The same explanation can be applied for the cases of 7 and 8 for the change of mold temperature.

As the packing pressure was increased while the other parameters were kept constant as shown in the case 9 through 12,  $x_c/L$  increased from 0.23 to 0.33 for the isotherm of 100°C and from 0.25 to 0.39 for the isotherm of 130°C, respectively, as shown in Table 5. The effect of the packing pressure on the first merging position of the frozen layers  $x_c/L$  was found to be much higher than for the center-gated disks.

Finally we have tested the effect of the cavity thickness on the first merging position of the

**Table 6** Molding conditions for rectangular plates.

Case No.	$T_M$ (°C)	$T_w$ (°C)	Flow Rate (cc/sec)	Packing Pressure (MPa)	100°C ( $x_c/L$ )	130°C ( $x_c/L$ )	Cavity Thickness (mm)
1	225	40	23.8	14.0	0.27	0.31	2.0
2	210	40	23.8	16.2	0.25	0.27	2.0
3	240	40	23.8	11.9	0.29	0.33	2.0
4	225	40	11.9	13.5	0.29	0.33	2.0
5	225	40	35.7	14.5	0.27	0.29	2.0
6	225	40	47.6	14.9	0.25	0.29	2.0
7	225	50	23.8	13.9	0.27	0.31	2.0
8	225	60	23.8	13.8	0.25	0.31	2.0
9	225	40	23.8	2.80	0.23	0.25	2.0
10	225	40	23.8	8.39	0.25	0.27	2.0
11	225	40	23.8	21.0	0.31	0.35	2.0
12	225	40	23.8	28.0	0.33	0.39	2.0
13	225	40	23.8	167.7	0.07	0.07	0.5
14	225	40	23.8	45.4	0.11	0.13	1.0
15	225	40	23.8	6.46	0.23	0.25	3.0
16	225	40	23.8	3.61	0.23	0.25	4.0

frozen layers  $x_c/L$  as shown in the case 13 through 16. Because the packing pressure should be decided from a certain rule the packing pressure has been kept constant as the pressure for the gate at the end of fill of the cavity. Note that, in the actual molding process, the packing pressure can be set with the pressure at the end of fill as a reference which guarantees no backflow.

For the cavity thickness of 0.5mm  $x_c/L$  for both 100°C and 130°C were only 0.07. It was due to the shear heating from the high shear rate in a very thin cavity. And  $x_c/L$  increased as the thickness increased until 2.0mm (case 1). However, for the cavity thicknesses of 3.0mm and 4.0 mm  $x_c/L$  decreased again to 0.23 for the isotherm of 100°C and 0.25 for the isotherm of 130°C, respectively, as shown in Table 5. It was very interesting numerical results to note.

#### 4. Discussion

We have focused on the effect of process conditions on the merging position of frozen layers for center-gated disks and rectangular plates. We

found that the frozen layers formed from both sides of cavity started to merge at about 0.75R from the center for the center-gated disks and about 0.25 - 0.35 L from the gate for the rectangular plates for most of process conditions.

For the cases of center-gated disks the change of melt temperatures or the packing pressure had little effect for the merging position of frozen layers. However, as the flow rate increased  $r_c/R$  decreased.

For the cases of rectangular plates as the melt temperatures increased  $x_c/L$  increased with a minor effect. However, as the flow rate increased  $x_c/L$  decreased as shown for the cases of center-gated disks.  $x_c/L$  showed almost linear increase as the packing pressure increased because more material entered the cavity in the postfilling stage. Finally, for the very thin cavity of 0.5mm an exceptionally small value of  $x_c/L$  was found. As the cavity thickness increased up to 2.0mm  $x_c/L$  increased, then it decreased for the cases of 3.0 and 4.0mm.

The present results could help to explain the overpacked region in injection-molded parts for

different geometries.

The maximum optical distortion was found almost at the same radial position, namely, 0.75R by Wimberger-Friedl (1990). This motivates the present study to find the correlation among the stress field, frozen layer and optical field. Further work is in progress to this direction.

### 5. Acknowledgment

This work is supported by Korea Science and Engineering Foundation (94-1400-04-01-3), for which the author is grateful. The author is also would like to thank Dr. C. A. Hieber and Professor K. K. Wang at Cornell university for their continuous supports and discussions in the course of study.

### References

- Baaijens, F. P. T., 1991, *Rheol. Acta.*, Vol. 30, p. 284.
- Bernhardt, E. C. (Ed.), 1983, *Application of Computer Aided Engineering in Injection Molding*, Hanser Publishers, Munich.
- Chiang, H. H., Hieber, C. A. and Wang, K. K., 1991a, *Polym. Eng. Sci.*, Vol. 31, p. 116.
- Chiang, H. H., Hieber, C. A. and Wang, K. K., 1991b, *Polym. Eng. Sci.*, Vol. 31, p. 125.
- Flaman, A. A. M., 1993a, *Polym. Eng. Sci.*, Vol. 33, p. 193.
- Flaman, A. A. M., 1993b, *Polym. Eng. Sci.*, Vol. 33, p. 202.
- Gilmore, G. D. and Spencer, R. S., 1950, *Modern Plastics*, Vol. 27, p. 143.
- Gilmore, G. D. and Spencer, R. S., 1951, *J. Colloid Sci.*, Vol. 6, p. 118.
- Huilier, D. G. F. et al., 1988, *Intern. Polym. Proc.*, Vol. 3, P. 184.
- Huilier, D. G. F., 1990, *J. of Polym. Eng.*, Vol. 9, p. 237.
- Kamal, M. R. and Kenig, S., 1972, *Polym. Eng. Sci.*, Vol. 12, p. 294.
- Isayev, A. I. and Hieber, C. A., 1980, *Rheol. Acta.*, Vol 19, p. 168.
- Isayev, A. I.(Ed.), 1987, *Injection and Compression Molding Fundamentals*, Marcel Dekker, New York.
- Isayev, A. I.(Ed.), 1991, *Modeling of Polymer Processing*, Hanser Publishers, Munich.
- Janeschitz-Kriegl, H., 1977, *Polymer Melt Rheology and Flow Birefringence*, Springer-Verlag, Berlin.
- Leonov, A. I., Lipkina, E. H., Pashkin, E. D. and Prokunin, A. N., 1976, *Rheol. Acta.*, Vol. 15, p. 411.
- Leonov, A. I., 1976, *Rheol. Acta.*, Vol. 15, p. 85.
- Manzoine, L. T.(Ed.), 1987, *Application of Computer Aided Engineering in Injection Molding*, Hanser Publication, Munich.
- Mavridis, H., Hrymak, A. N. and Vlachopoulos, J., 1988, *J. of Rheol.*, Vol. 32, p. 639.
- Patankar, S. V., 1980, *Numerical Heat Transfer and Fluid Flow*, Hemisphere, New York.
- Wang, K. K. et al., 1992, *Cornell Injection Molding Program*, Progress Report 16, Cornell University.
- Yoon, K. and Wang, K. K., 1992, *SPE Tech. Paper*, Vol. 32, p. 2221.
- Wimberger-Friedl, R., 1990, *SPE Tech. Paper*, Vol. 30, p. 813.